

## **Fabrication of Activated Carbon from Coconut Shells and its Electrochemical Properties for Supercapacitors**

*S. M. Omokafe<sup>1,4</sup>, A.A. Adeniyi<sup>1</sup>, E. O. Igbafen<sup>1</sup>, S. R. Oke<sup>2,3\*</sup>, P.A. Olubambi<sup>4</sup>*

<sup>1</sup> Department of Metallurgical & Materials Engineering, Federal University of Technology Akure, PMB 704, Nigeria.

<sup>2</sup> Department for Management of Science and Technology Development, Ton Duc Thang University, Ho Chi Minh City, Vietnam

<sup>3</sup> Faculty of Civil Engineering, Ton Duc Thang University, Ho Chi Minh City, Vietnam

<sup>4</sup> Centre for Nanoengineering and Tribocorrosion, University of Johannesburg, Johannesburg, South Africa

\*E-mail: [samuel.ranti.oke@tdtu.edu.vn](mailto:samuel.ranti.oke@tdtu.edu.vn)

\*Corresponding author at: Ton Duc Thang University, Ho Chi Minh City, Vietnam

*Received: 7 April 2020 / Accepted: 18 May 2020 / Published: 30 September 2020*

---

The problem posed by the use of fossil fuel energy and the increase in cost for energy storage materials, has led to the development of considerably cheap and environmentally friendly materials for energy storage. This has increased interest in biomass materials for synthesis of activated carbons, particularly as electrode materials for supercapacitor. For this research, coconut shell was utilized as a precursor material for the fabrication of activated carbon due to its availability, high carbon content, and the problem its disposal poses on the environment. Coconut shells were sourced locally, heated in a furnace, and activated using a two-step chemical activation with 1M H<sub>2</sub>SO<sub>4</sub> and 1M KOH. The activated carbon was compacted and subjected to a cyclic voltammetry test using varied scan rates of 20, 40, 60, 80 and 100 mV/s, and a potential window between 0.05 and 0.8. The specific capacitance at scanning rates of 20, 40, 60, 80 and 100 mV/s are 600.89, 299.78, 378.31, 374.13, and 286.92 F/g respectively. The highest specific capacitance of 600.89 F/g and energy density of 46.94 Wh/kg was obtained at a scan rate of 20 mV/s. When compared with previous studies, the synthesized activated carbon electrodes from this research had the highest specific capacitance.

---

**Keywords:** Activated carbon; Coconut shell; Supercapacitor; Energy storage; Electrode

### **1. INTRODUCTION**

Environmental issues and the high cost of petrochemical feedstock have shifted research towards renewable and sustainable resources for generation and storage of energy [1]. The utilization of supercapacitors as energy storage devices in electronics, energy, transportation and aviation industries

have gained attention over the years [2, 3]. This is due to their excellent stability, ultra-fast charge and discharge rates, high energy density and long-term cycle life. Based on electrode material types, supercapacitors are classified into three: conductive polymers such as polyaniline and polypyrrole (PPy); Manganese and Ruthenium based metal oxides; and carbon-based materials [4, 5]. The polymer and metal oxide-based electrodes possess attractive properties such as high charge capacity, good stability and high conductivity, but are produced at relatively high costs with limited production rates [6, 7]. This has increased the interest in the utilization of biomass materials for fabrication of activated carbons for supercapacitor application.

In the last decade, research interests have been targeted towards the search and development of alternative and cost effective carbon materials [8]. Porous carbon sources offer major potential alternatives mainly because of their cost effectiveness, abundance, and environmentally friendliness. They possess distinctive and attractive properties as a result of their high absorption capability, microporous structure, extended surface area, and high degree of surface reactivity [9]. The usage of biomass materials for the preparation of porous activated carbons electrode materials for supercapacitors have attracted extensive attention [10]. Agricultural waste materials such as orange peel [11], palm kernels [12], rice husk [13], banana peel [14], pineapple leaf fiber [15] have been utilized in various researches for synthesizing activated carbon due to their low cost.

Among agro-waste materials used as electrodes for supercapacitors, activated carbon of coconut shell origin have been documented to be of enhanced quality compared to other sources [16]. Its high conductivity, mesoporous structure, and large surface area makes it appropriate for utilization as electrode material [17, 18]. Economically, coconut shells have no value, its disposal is expensive and may cause problems to the environment. Li et al. [19] utilized a single step thermal treatment followed by steam activation to produce activated carbon from coconut shell. The authors affirmed enhanced performance of the activated carbon for supercapacitors but reported poor cycle stability. Juan et al. [20] also fabricated a high performance porous activated carbon from coconut shell for application as supercapacitors using one-step thermal treatment and steam activation. The activated carbons also exhibit enhanced electric conductivity. Chemical activation procedures for the synthesis of activated carbon from coconut shell have been reported [21]. High-surface-area coconut shell based activated carbons was fabricated by Hu and Srinivasan [22] using KOH as activation agent. Similar work on the synthesis of coconut shell based activated carbon using KOH as an activating agent have also been reported [17]. The use of  $ZnCl_2$  as activation agent for microporous activated carbon from coconut shells have also been reported [16].

In this study, we prepared a coconut shell based activated carbon electrodes using a 2-stage chemical activation process with  $H_2SO_4$  and KOH. The porous structure and energy storage capacity of the activated carbon electrodes were investigated. The novelty of the study is the use of a two-stage chemical activation method for synthesizing activated carbon of coconut shell origin. Other works have only relied on a physical followed by a chemical activation method and vice versa.

## 2. EXPERIMENTAL

### 2.1. Preparation of activated carbon

#### 2.1.1 Sourcing and preparation of activated carbon

Locally sourced coconut shells were crushed into smaller pieces of about 5 mm each after drying. This was done in order to increase the efficacy of the pyrolysis process by creating large surface area for carbonization. The crushed shells were washed and filtered to get rid of dust particles and other solid impurities. The coconut shells were then heated at 100 °C for 2 hours in an electric oven.

#### 2.1.2 Pyrolysis of crushed carbon

The crushed and dried coconut shell samples were fed into a medium sized reactor; a tightly lidded crucible in vacuum electric furnace for pyrolysis. Each charge was heated at 600 °C for 12 hours to facilitate the pyrolysis. The pyrolysed lumps were then transferred to a ball mill and milled for about 2 hours. The milled samples were sieved and the oversized particles reground until the entire charge was in the -300 µm size range.

#### 2.1.3 Two stage (acid-alkali) chemical activation

The sieved particles of pyrolysed carbon were poured in beakers containing 1M H<sub>2</sub>SO<sub>4</sub>. The resulting mixture was then stirred using a glass rod and left to soak for 2 hours. The acid activated carbon material was repeatedly rinsed in distilled water and transferred into beakers containing 1M KOH solution for the second (alkali) stage of the activation. The mixture was again stirred, soaked for 2 hours, repeatedly rinsed with distilled water and finally dried at 100 °C in the oven for 2 hours.

### 2.2. Fabrication of activated carbon supercapacitor electrode

Following activation, the activated carbon was taken to the ball mill, where it was milled for about 1 hour. The activated carbon samples were sieved to a size less than 106 µm. Polyvinyl alcohol (PVA) was selected as a suitable binder due to its mechanical strength, wettability and capacitance, which was greater when compared to polyvinylidene fluoride (PVDF) [23]. 1g of PVA was mixed with 75 mL of distilled water. The solution was stirred for about 20 minutes at room temperature. After that, 30g of activated carbon was mixed with the prepared solution and stirred for 2 hours. The paste was coated and mounted into a castable polymer material. Finally, carbon electrode was allowed to dry.

### 2.3. Structural Characterization

Samples of the fabricated acid-alkali activated carbon electrodes were characterized to identify the elements, functional groups and their structures. This was done via scanning electron microscopy (SEM), X-ray diffraction (XRD), and Energy Dispersive X-ray spectroscopy (EDX). A JEOL JSM-7600F SEM was used to investigate the morphology and apparent porosity of the developed electrode

after acid-alkali activation of the coconut shell derived carbon. EDX was used to deduce the elemental composition of the carbon electrode. XRD was used to analyse and identify the other non-carbon compounds still present on the electrode surface after the activation process. The sample was analyzed using Rigaku D/Max-III C X-ray diffractometer developed by the Rigaku Int. Corp. Tokyo, Japan. Diffractions were produced at scanning rate of  $2^\circ/\text{min}$  in  $2^\circ$  to  $50^\circ$  at room temperature with a Cu-K $\alpha$  radiation set at 40 kV and 20 mA.

## 2.4. Electrochemical Evaluation

### 2.4.1 Cyclic Voltammetry

Cyclic voltammetry was carried out to assess the charge storage/supercapacitor properties of the developed acid-alkali activated coconut shell carbon electrode. Samples were affixed with copper conductors and cold mounted on a polyester base to hold the conductor in place. Each sample was immersed in a three-electrode electrochemical cell consisting of the mounted sample, a Ag/AgCl reference electrode and a platinum counter electrode and a 1M  $H_2SO_4$  solution as electrolyte. The electrodes were connected to a Versastat 4 potentiostat. The electrodes were subjected to three (3) cycles of cyclic voltammetry from 0.05V to 0.8V potential window at 20, 40, 60, 80 and 100 mV/s scan rates respectively. The charge storage parameters such specific capacitance  $C_{sp}$  and energy density  $E$  were then determined. The specific capacitance of the acid-alkali coconut shell derived activated carbon electrode was calculated from the CV chart using equation (1).

$$C_{sp} = \frac{Q}{\Delta V * \partial v / \partial t * m} \quad (1)$$

Where Q is the area within the CV curve,  $\partial v / \partial t$  is the applied scan rate,  $\Delta V$  is the potential window and m is the mass of the activated carbon electrode.

The Energy density was calculated using equation (2).

$$E = C_{sp} * \frac{\Delta V^2}{7.2} \quad (2)$$

### 2.4.2 Electrochemical impedance spectroscopy (EIS)

Electrochemical impedance spectroscopy was used in this work to investigate the nature of the interactions that occur at the electrode-electrolyte interface. The procedure used was akin to that followed during the cyclic voltammetry. The setup was allowed about 1 hour to establish open circuit potential. The electrode was subjected to 10 mV amplitude of alternative signals at open circuit from 0.1 Hz to 100 KHz. The obtained readings were plotted on nyquist and bode plots. The resulting nyquist plot was fitted using a proprietary EIS fitting software. Relevant parameters such as the charge transfer resistance and power density of the developed electrode were determined.

### 3. RESULTS AND DISCUSSION

#### 3.1 Morphological analysis

Figure 1(a-c) shows micrographs of the developed acid-alkali activated carbon electrode at 20  $\mu\text{m}$  and 5000x, 6000x, and 8000x magnifications respectively. Figure 1(a-c) reveals that the two-stage acid-alkali activation treatments resulted in an activated carbon electrode with an enhanced porous structure. Magnified images of the microstructures (Fig. 1c) shows completely opened cell pores on the electrodes surface. The high levels of pore opening signify larger surface area and increased number of reaction sites on the activated carbon electrode. Larger surface areas have been reported to improve charge storage capabilities of electrodes due to more effective electro-adsorption processes [24]. The formation of pore as observed in the Fig. is attributed to the synergistic effects of the acidic and alkali chemical activation processes. The acidic activation stage using  $\text{H}_2\text{SO}_4$  helps to create more pores by the dissolution of the constituent metallic atoms which are randomly intercalated within the bulk carbon material while the alkali activation using  $\text{KOH}$  thus helps to dissolve organic residues left in the carbonized material. In a related work by Jain and Tripathi [17], pore formation was attributed to the release of volatile matter and activating agents from the sample. They also reported enhanced utilization ratio of active substances due to large surface area.

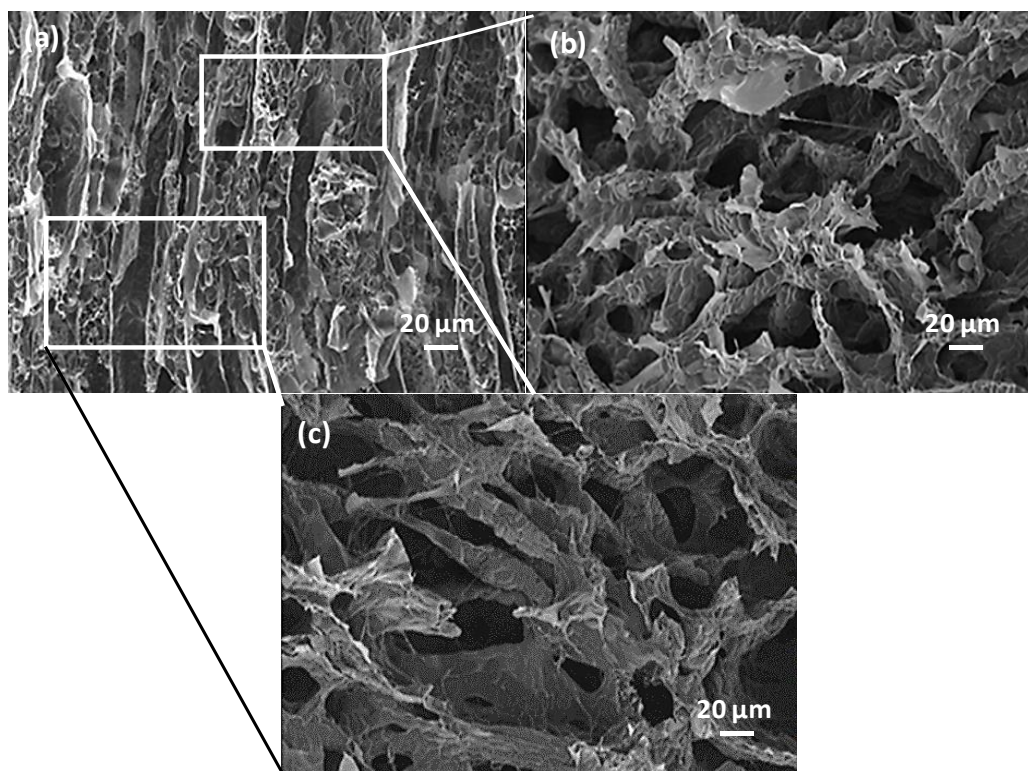


**Figure 1.** SEM micrographs obtained at different magnifications (a) 8000x (b) 6000x (c) 5000x

### 3.2 Elemental analysis

The EDX microanalysis (Figure 2) of the activated carbon electrode revealed it contained about 70.00 % carbon, 9.27 % oxygen, 15.55 % hydrogen, 3.70 % sulfur, around 1.48 % of iron relatively. The works of authors such as [25] showed that dry and unprocessed coconut shells contain only about 59 wt.% Carbon. As shown in the EDX in Figure 2, the developed activated carbon electrode contained up to 70 wt. % Carbon. The acid-alkali activation greatly increased the proportion of carbon in the biomass (coconut shell) material from pre-activation levels. The increment in proportion of carbon in the activated carbon electrode from pre-activation amounts can be attributed to the removal of metallic and non-metallic constituents in the original lignocellulosic biomass material by the H<sub>2</sub>SO<sub>4</sub> and KOH activation processes.

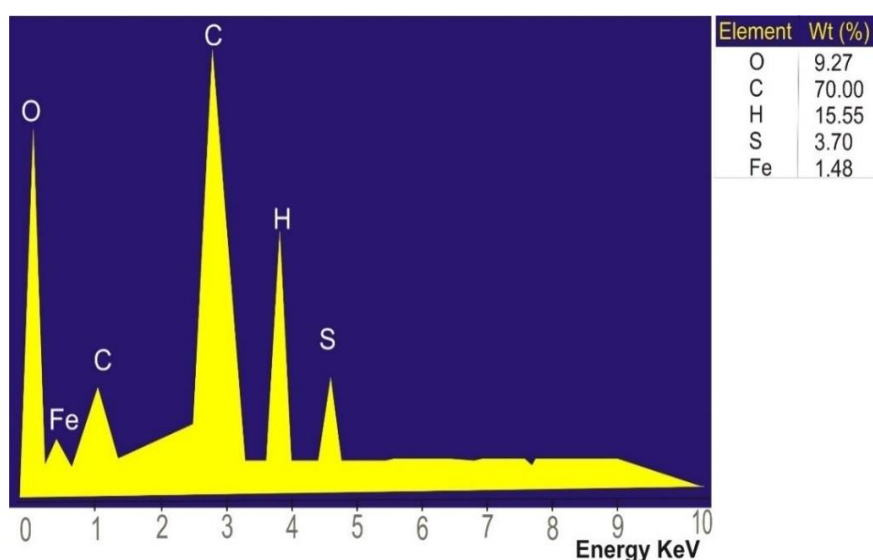


**Figure 2.** EDX of activated carbon from coconut shells

The XRD pattern in Figure 3 depicts the different compounds present in significant amounts in the activated carbon electrode synthesized from coconut shell. The pattern reveals that the carbon electrode contains compounds of calcium, aluminium, magnesium and silicon in addition to the oxygen, carbon, hydrogen, sulphur and iron revealed in the EDX. The compounds are present in simple, double and/or complex oxides and sulphides forms. Their presence may be attributed to the remnants of these substances which remained in the starting materials after the activation process. The impurities may contribute to local action when the electrode is immersed in an electrolyte, contributing to the electrode's internal resistance. The EDX does not show some of the elements identified in the XRD because these elements may only be present in extremely small amount and thus negligible quantities that lie below the sensitivity of the EDX. The two-stage activation process is responsible for the significant reduction in the proportion of non-carbon elements in the electrode. This supports the suitability of the two step (acid-alkali) chemical activation method.

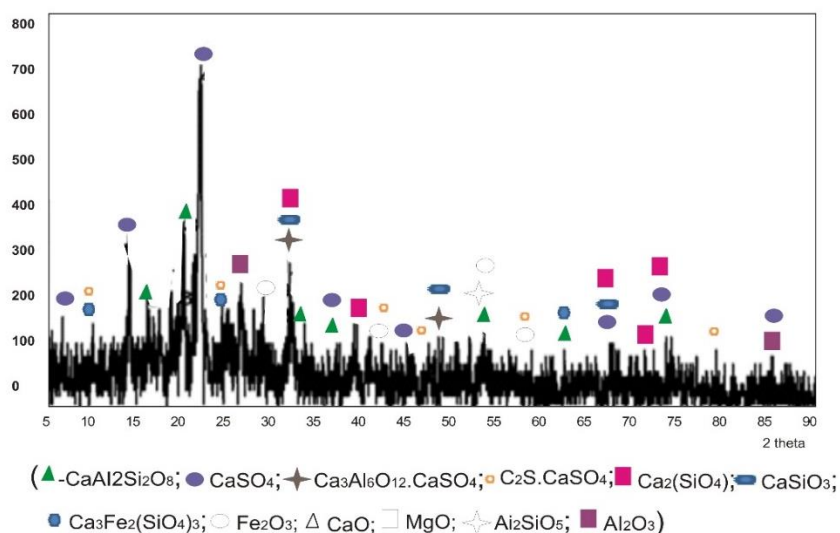


**Figure 3.** XRD pattern for coconut shells activated carbon

### 3.3 Electrochemical Evaluation of coconut shell derived activated carbon Electrode Performance

Figure 4 shows the cyclic voltammograms (CV) obtained when the developed acidic-alkali activated carbon electrode derived from coconut shells was immersed in an electrolytic cell at 20, 40, 60, 80 and 100 mV/s within 0.05 – 0.8V potential window (Ag/AgCl). The CV curves are mostly identical in shape even at higher scan rates. The similarity in the shape of CV plots at most scan rates may infer that the same or similar electrolytic reactions occur in the cell irrespective of the scan rate employed. This indicates enhanced charge transfer stability of the device. All the CV curves appear as quasi-rectangular/hysteretic structures, this indicates good charge storage and capacitive capability. Such semi rectangular cyclic voltammetry curves indicate good capacitance behavior of the electrode [26]. The spikes on the curves may be attributed to electrical noise or the occurrence of numerous intermediate reactions in the charging/storage and discharge phases of the electrolytic cell. The 60 mV/s electrode exhibited this behaviour the most. The CV curves are mostly closed on both ends, this may infer the electrode's capability for complete reversibility between charging and discharge. Thus, attesting to the stability of the developed electrode as can be observed with the 20 and 40 mV/s electrodes.

Table 1 shows the corresponding specific capacitance and energy densities for each scan rate. The specific capacitance and energy density were noted to majorly decrease with increase in scan rate. The highest capacitance value of 600.89 F/g and energy density of 46.94 Wh/Kg was obtained from the 20mV/s scan rate electrode. This may be because low scan rates allow for adequate diffusion of ions into and from the pores of the electrodes, which is crucial for the formation of stable electrochemical double layers. This implies that the electrodes surface adsorbs more ions/charges, this indicates better capacitive behavior. The capacitor electrode efficiency improves with decrease in scan rates rate.

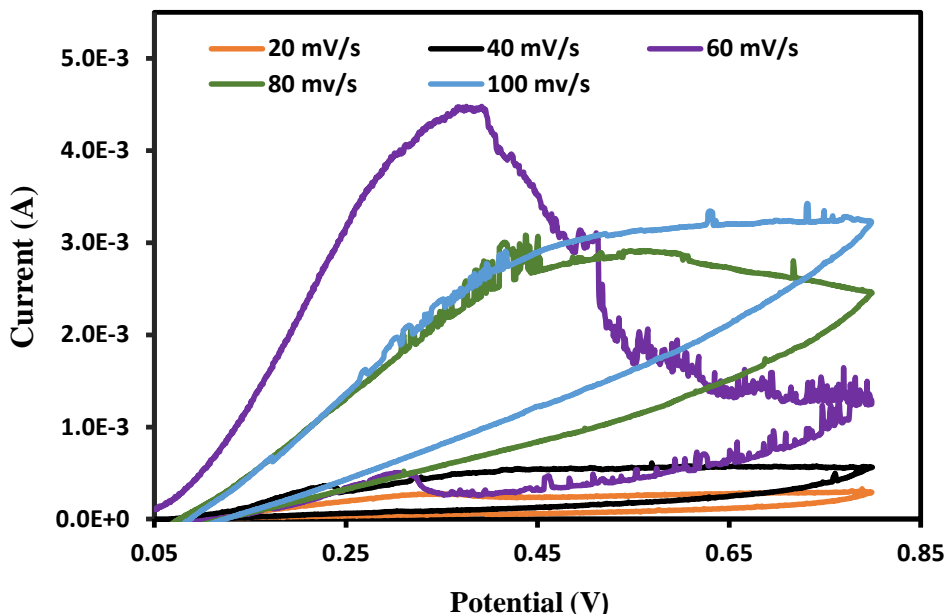


**Figure 4.** CV graphs of the activated carbon obtained at different scan rates

**Table 1.** Variation of energy density and specific capacitance with scan rate for acid-alkali activated carbon electrode derived from coconut shell

Scan rate (mV/s)	Specific Capacitance (F/g)	Energy density (Whkg <sup>-1</sup> )
20	600.89	46.94
40	299.78	23.42
60	378.31	29.56
80	374.13	29.78
100	286.92	22.38

Electrochemical impedance spectroscopy allowed for more detailed insight into the electrochemical performance of the developed activated carbon electrode. The Nyquist and Bode plots of the EIS procedure are presented in Figure 5 and Figure 6 respectively. The Nyquist plots shown in Figure 5 shows that the activated carbon electrode exhibits capacitance and conductive features at the electrode-electrolyte interface. Given the nature of the nyquist plot obtained, the equivalent circuit shown in Figure 7 was drawn to represent the features at the electrode-electrolyte interface. It was drawn with proteus 8<sup>TM</sup>, a proprietary circuit analysis software. The nyquist plots shows the features of a simple randle’s circuit. The Rs denotes the solution resistance whereas Rct denotes the resistance to charge transfer. The resistance to charge transfer is an indicator of the inherent internal resistance of the developed activated carbon electrode. It is obtained from the difference between the intercepts of the nyquist curve on the Z’ axis. That is, the diameter of the nyquist semicircle represents the charge transfer resistance at the electrochemical double layer and is related to the electronic resistance of the electrode. The significant value of charge transfer (internal) resistance shown by the electrode can be linked to the

effect of impurities present electrode. Impurities serve to alter the surface reactivity of the electrode particles [27] and may trigger undesirable intermediate reaction(s), thus reducing the efficiency electrode and electrochemical cell or supercapacitor. The nyquist plot takes the shape of a depressed semicircle, this indicates the capacitive nature of the electrochemical double layer at the activated carbon electrode-electrolyte interface, thus confirming the suitability of the developed electrode to perform in such (supercapacitor) applications.

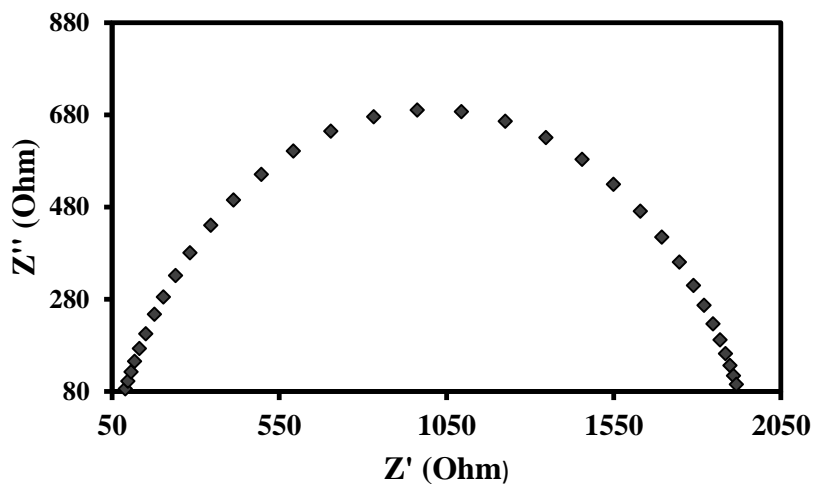


**Figure 5.** Nyquist plot of from the electrochemical impedance spectroscopy of an electrochemical cell with the activated carbon electrode.

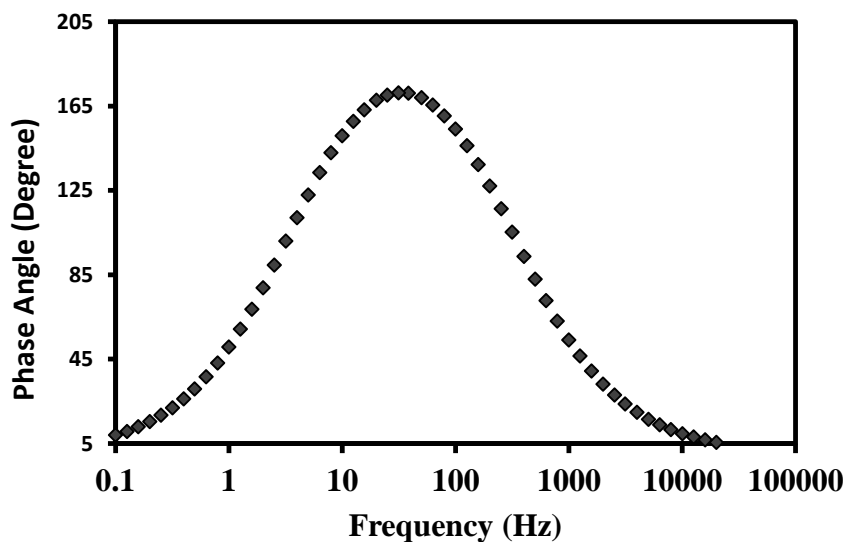


**Figure 6.** EIS Bode Plot of activated carbon electrode in the Electrochemical cell

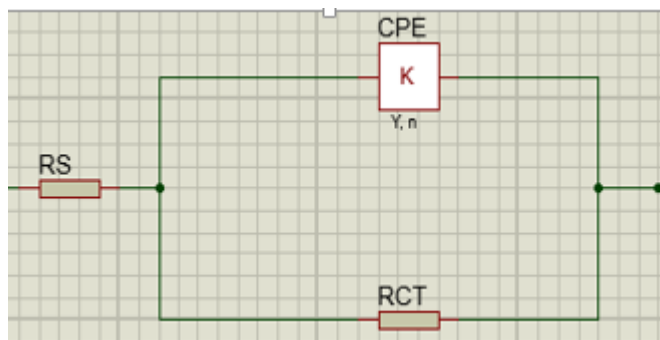


**Figure 7.** Selected equivalent circuit representing the nature of the activated carbon electrode-electrolyte interface in the electrochemical cell.

### 3.4 Comparison of the present study with those obtained using coconut shell

The specific capacitance and energy densities of earlier studies using coconut shell based activated carbon were compared with data gotten from our study. The comparisons are presented in Table 2. The variance in the capacitance and energy density values can be partly attributed to the different methods adopted for the synthesis of the activated carbon. It is evident from the table that the specific capacitance obtained from this present study is higher than most of those reported using other activation methods.

**Table 2.** Comparison of the present study with those obtained using coconut shell

Agro-Waste	Activation Method	Capacitance (F/g)	Energy density Whkg <sup>-1</sup>	Reference
Coconut shell	Physical, steam, 200 °C/30 - 90 min	228.00	38.50	[20]
Coconut shell	Chemical, ZnCl <sub>2</sub> , FeCl <sub>3</sub> under N <sub>2</sub> atmosphere	210-268	54.70	[19]
Coconut shell	Chemical, ZnCl <sub>2</sub> physical CO <sub>2</sub>	159.00	69.00	[28]
Coconut shell	Self-activation using the pyrolysis gases	258.00	-	[29]
Coconut shell	Chemical, KOH	356.20	88.80	[17]
Coconut shell	2 stage chemical activation with H <sub>2</sub> SO <sub>4</sub> followed by KOH.	600.89	46.94	This work

Although, a higher energy density (lower specific capacitance compared to our work) has been reported by [16], the team used sodium thio-cyanate (NaSCN), which apart from being a toxic substance also releases a very toxic gas especially when in contact with acids. Moreover, the pyrolysis time was about 5 hours and the chemical activation process involved much longer time of 18-20 hours compared to our own which took less than 3 hours. Finally, the concentration of KOH was higher and their process

included the use of  $\text{CaCl}_2$  both of which would significantly increase the costs involved. Hence, their reported energy density of 88.8 Wh/Kg compared to our own 46.94 Wh/Kg. The Energy density reported in this study is also a little lower compared to those prepared using  $\text{ZnCl}_2$  chemical activation, albeit the lower cost of our own procedure. Compared to other activated carbon electrode preparation procedures such as those involving physical and steam activation (38.5 Wh/Kg), our procedure yielded better results in this aspect.

From the results presented, it is imperative to state that activated carbon electrodes of high specific capacitance and energy density can be processed from coconut shells using simpler, safer and lower cost 2-stage chemical activation with  $\text{H}_2\text{SO}_4$  followed by KOH treatment.

#### 4. CONCLUSIONS

This paper successfully demonstrated high performance and porous activated carbon material synthesized by pyrolysis and KOH,  $\text{H}_2\text{SO}_4$  (acid-alkali) chemical activation of coconut shells, which is an abundant resource in many developing countries. The developed activated carbon electrode possessed significantly high charge storage capacity, reaching up to 600.89 F/g and Energy density reaching up to 46.94 Wh/kg. The carbon electrodes exhibited good stabilities with moderate charging and discharge cycles. Our studies indicated that the coconut shell derived carbon are promising materials for improved performance supercapacitor devices. In all, coconut shell derived activated carbon shows favorable electrical properties and a high capacitance. It therefore offers good potential as precursor for activated carbon in the production of supercapacitor electrodes and acid-alkali chemical activation procedure is sufficient to obtain optimum properties from the developed electrode.

#### References

1. C. Ranaweera, P. Kahol, M. Ghimire, S. Mishra and R.K. Gupta, *C—J. of Carbon Research*, 3 (2017) 25.
2. D.O. Akinyele and R.K Rayudu, *Sustainable Energy Technol. Assess.*, 8 (2014) 76.
3. B.K. Kim, S. Sy, A. Yu, J. Zhang, *Handbook of Clean Energy Systems*, (2015) 2.
4. H. Feng, L. Tang, G. Zeng, J. Tang, Y. Deng, M. Yan, Y. Liu, Y. Zhou, X. Ren and S. Chen, *J. Mater. Chem. A*, 6 (2018) 7310.
5. J. Yang, Y. Liu, S. Liu, L. Li, C. Zhang and T. Liu, *Mater. Chem. Front.*, 1 (2017) 252.
6. W. Wei, X. Cui, W. Chen and D.G. Ivey, *Chemical society reviews*, 40 (2011) 1697.
7. A. Yağan, *Int. J. Electrochem. Sci.*, 14 (2019) 3979.
8. K. Mensah-Darkwa, C. Zequine, P.K. Kahol and R.K. Gupta, *Sustainability*, 11 (2019) 414.
9. L.J. Kennedy, T. Ratnaji, N. Konikkara and J.J. Vijaya, *J. Cleaner Prod*, 197 (2018) 930.
10. A. Jain, R. Balasubramanian and M. Srinivasan, *Chem. Eng. J.*, 283 (2016) 790.
11. M. Dhelipan, A. Arunchander, A. Sahu and D. Kalpana, *J. of Saudi Chem. Soc.*, 21 (2017) 488.
12. F.O. Aramide and S.R. Oke, *Acta Technica Corviniensis-Bulletin of Eng.*, 7 (2014) 133.
13. E.Y.L. Teo, L. Muniandy, E.P. Ng, F. Adam, A.R. Mohamed, R. Jose and K.F. Chong, *Electrochim. Acta* 192 (2016) 112.
14. E. Taer, R. Taslim, Z. Aini, S. Hartati and W. Mustika, *AIP Conference Proceedings*, (2017) 040004.
15. S. Baru, *Int. J. Electrochem. Sci.*, 14 (2019) 2464.

16. D.C. Azevedo, J.C.S. Araujo, M. Bastos-Neto, A.E.B. Torres, E.F. Jaguaribe and C.L. Cavalcante, *Microporous Mesoporous Mater.*, 100 (2007) 362.
17. A. Jain and S. Tripathi, *Mater. Sci. Eng., B*, 183 (2014) 58.
18. E. Taer, R. Taslim, A. Putri, A. Apriwandi and A. Agustino, *Int. J. Electrochem. Sci.*, 13 (2018) 12073.
19. L. Sun, C. Tian, M. Li, X. Meng, L. Wang, R. Wang, J. Yin and H. Fu, *J. Mater. Chem. A*, 1 (2013) 6463.
20. J. Mi, X.R. Wang, R.J. Fan, W.H. Qu and W.C. Li, *Energy Fuels*, 26 (2012) 5323.
21. S. Guo, J. Peng, W. Li, K. Yang, L. Zhang, S. Zhang and H. Xia, *Appl. Surf. Sci.*, 255 (2009) 8443-8449.
22. Z. Hu and M. Srinivasan, *Microporous Mesoporous Mater.*, 27 (1999) 14.
23. Y.J. Zhang, J. Guo, and T. Li, *Trans. Tech. Publ.*, (2012) 783.
24. A. Borenstein, O. Hanna, R. Attias, S. Luski, T. Brousse and D. Aurbach, *J. Mater. Chem. A*, 5 (2017) 12653.
25. W.M.A.W. Daud and W.S.W. Ali, *Bioresour. Technol.*, 93 (2004) 66.
26. K. Jurewicz, S. Delpoux, V. Bertagna, F. Beguin and E. Frackowiak, *Chem. Phys. Lett.*, 347 (2001) 38.
27. W. Raza, F. Ali, N. Raza, Y. Luo, K.H. Kim, J. Yang, S. Kumar, A. Mehmood and E.E. Kwon, *Nano Energy*, 1 (2018) 441.
28. A. Jain, V. Aravindan, S. Jayaraman, P.S. Kumar, R. Balasubramanian, S. Ramakrishna, S. Madhavi and M. Srinivasan, *Sci. Rep.* 3 (2013) 4.
29. K. Sun, C.-y. Leng, J.-c. Jiang, Q. Bu, G.-f. Lin, X.-c. Lu, G.-z. Zhu, *Carbon*, 130 (2018) 844.